Chapter 7

Topological Hypothesis on the Origin of Phase Transitions

In the previous chapter we have reported results of numerical simulations for the fluctuations of observables of a geometric nature (e.g., configuration-space curvature fluctuations) related to the Riemannian geometrization of the dynamics in configuration space.[1] These quantities have been computed, using time averages, for many different models undergoing continuous phase transitions, namely φ^4 lattice models with discrete and continuous symmetries and XY models. In particular, when plotted as a function of either the temperature or the energy, the fluctuations of the curvature have an apparently singular behavior at the transition point. Moreover, we have seen that the presence of a singularity in the statistical-mechanical fluctuations of the curvature at the transition point has been proved analytically for the mean-field XY model.

The aim of the present chapter is to try to understand on a deeper level the origin of this peculiar behaviour. In Section 7.1, we will show, using abstract geometric toy models, that a singular behavior in the fluctuations of the curvature of a Riemannian manifold can be associated with a change in the *topology* of the manifold itself. By "change of topology" we mean the following. Let us consider a surface $\mathcal{S}_\varepsilon$ that depends on a parameter ε in such a way that upon varying the parameter, the surface is continuously deformed: as long as the different deformed surfaces can be mapped *smoothly* one onto another,[2] the topology does not change; however, the topology changes if there is a critical value of the parameter, say ε_c, such that the surface $\mathcal{S}_{\varepsilon>\varepsilon_c}$ can no longer be mapped smoothly onto $\mathcal{S}_{\varepsilon<\varepsilon_c}$.

The observation that a singularity in the curvature fluctuations of a Riemannian manifold, of the same type as those observed numerically at phase transitions, can be associated with a change in the topology of the manifold leads us to conjecture that it is just this mechanism that could be the basis

[1] More precisely, we considered the enlarged configuration space-time, endowed with the Eisenhart metric.

[2] The different surfaces are then said to be diffeomorphic to each other (see Appendix A).

of thermodynamic phase transitions. Such a conjecture was originally put forward in [92] as follows: a thermodynamic transition might be related to a change in the topology of the configuration space, and the observed singularities in the statistical-mechanical equilibrium measure and in the thermodynamic observables at the phase transition might be interpreted as a "shadow" of this major topological change that happens at a more basic level. We will refer to this conjecture as the *topological hypothesis (TH)*.

In a first part of this chapter, we report about the logical path that, through heuristic and indirect evidence, led us to formulate the TH. In the second part of this chapter, a first *direct* numerical support to the validity of the TH is given for a specific model.

7.1 From Geometry to Topology: Abstract Geometric Models

Let us now describe how a singular behavior of the curvature fluctuations of a manifold can be put in correspondence with a change in the topology of the manifold itself. For the sake of clarity, we shall first discuss a simple example concerning two-dimensional surfaces [90, 92], and then we will generalize it to the case of N-dimensional hypersurfaces [194, 195].

The simple geometric model we are going to describe concerns surfaces of revolution. A surface of revolution $\mathbb{S} \in \mathbb{R}^3$ is obtained by revolving the graph of a function f around one of the axes of a Cartesian plane, and can be defined, in parametric form, as follows [196]:

$$\mathbb{S}(u,v) \equiv (x(u,v), y(u,v), z(u,v)) = (a(u)\cos v, a(u)\sin v, b(u)) \ , \qquad (7.1)$$

where either $a(u) = f(u)$ and $b(u) = u$, if the graph of f is revolved around the vertical axis, or $a(u) = u$ and $b(u) = f(u)$, if the graph is revolved around the horizontal axis; in both cases, u and v are local coordinates on the surface $\mathbb{S}$: $v \in [0, 2\pi]$ and u belongs to the domain of definition of the function f.

Let us consider now in particular the two families of surfaces of revolution defined as

$$\mathcal{F}_\varepsilon = (f_\varepsilon(u)\cos v, f_\varepsilon(u)\sin v, u) \qquad (7.2)$$

and

$$\mathcal{G}_\varepsilon = (u\cos v, u\sin v, f_\varepsilon(u)) \ , \qquad (7.3)$$

where

$$f_\varepsilon(u) = \pm\sqrt{\varepsilon + u^2 - u^4} \ , \qquad \varepsilon \in [\varepsilon_{\min}, +\infty) \ , \qquad (7.4)$$

and $\varepsilon_{\min} = -\frac{1}{4}$. Some cases are shown in Figure 7.1.

There exists for both families of surfaces a critical value of ε, $\varepsilon_c = 0$, corresponding to a change in the *topology* of the surfaces: the manifolds $\mathcal{F}_\varepsilon$ are diffeomorphic to a torus $\mathbb{T}^2$ for $\varepsilon < 0$ and to a sphere $\mathbb{S}^2$ for $\varepsilon > 0$; the manifolds $\mathcal{G}_\varepsilon$ are diffeomorphic to *two* spheres for $\varepsilon < 0$ and to one sphere

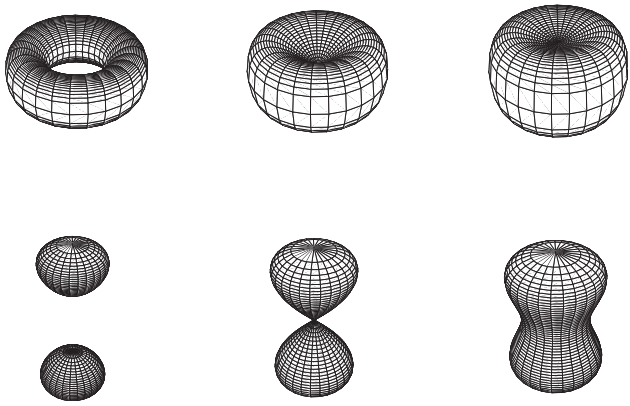

Fig. 7.1. Some representatives of the two families of surfaces $\mathcal{F}_\varepsilon$ and $\mathcal{G}_\varepsilon$ defined in (7.2) and (7.3) respectively. Each family is divided into two subfamilies by the critical surface corresponding to $\varepsilon_c = 0$ (middle members in the picture). Members of the same subfamily are diffeomorphic, whereas the two subfamilies are not diffeomorphic to each other. From [90].

for $\varepsilon > 0$. The Euler–Poincaré characteristic (see Appendix A) is $\chi(\mathcal{F}_\varepsilon) = 0$ if $\varepsilon < 0$, and $\chi(\mathcal{F}_\varepsilon) = 2$ otherwise, while $\chi(\mathcal{G}_\varepsilon)$ is 4 or 2 for ε negative or positive, respectively.

We now turn to the definition and the calculation of the curvature fluctuations on these surfaces. Let M belong to one of the two families; its Gaussian curvature K is [196]

$$K = \frac{a'(a''b' - b'a'')}{a(b'^2 + a'^2)^2} \ , \tag{7.5}$$

where $a(u)$ and $b(u)$ are the coefficients of (7.1), and primes denote differentiation with respect to u. The fluctuations of K can be then defined as

$$\sigma_K^2 = \langle K^2 \rangle - \langle K \rangle^2 = A^{-1} \int_M K^2 \, dS - \left(A^{-1} \int_M K \, dS \right)^2 \ , \tag{7.6}$$

where A is the area of M and dS is the invariant surface element. Both families of surfaces exhibit a singular behavior in σ_K as $\varepsilon \to \varepsilon_c$, as shown in Figure 7.2, in spite of their different curvature properties on average.[3]

We are now going to show that the result we have just obtained for two-dimensional surfaces has a much more general validity: a *generic* topology change in an n-dimensional manifold is accompanied by a singularity in its curvature fluctuations [194]. In order to do that, we have to make use of some concepts belonging to Morse theory, which will also be used in Section 7.4 below; the basic elementary concepts of Morse theory are sketched in

[3] For instance, $\langle K \rangle(\varepsilon) = 0$ for $\mathcal{F}_\varepsilon$ as $\varepsilon < 0$, while for $\mathcal{G}_\varepsilon$ the same average curvature is positive and diverges as $\varepsilon \to 0$.

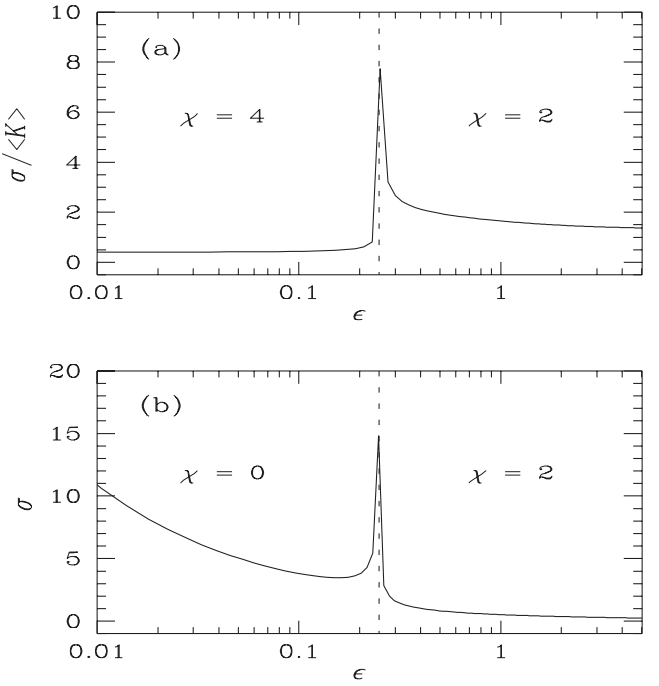

Fig. 7.2. The fluctuation σ of the Gaussian curvature of the surfaces $\mathcal{F}_\varepsilon$ and $\mathcal{G}_\varepsilon$ is plotted vs. ε; σ is defined in (7.6), and ε is shifted by $\varepsilon_{\min} = 0.25$ for reasons of clarity of presentation. (a) refers to $\mathcal{G}_\varepsilon$ and (b) refers to $\mathcal{F}_\varepsilon$. The cusps appear at $\varepsilon = 0$, where the topological transition takes place for both $\mathcal{F}_\varepsilon$ and $\mathcal{G}_\varepsilon$. From [90].

Appendix C, where also references to the literature are given. We consider then a hypersurface of $\mathbb{R}^N$ which is the u-level set of a function f defined in $\mathbb{R}^N$, i.e., a submanifold of $\mathbb{R}^N$ of dimension $n = N-1$ defined by the equation

$$f(x_1, \ldots, x_N) = u \ ; \tag{7.7}$$

such a hypersurface can then be referred to as $f^{-1}(u)$. Let us now assume[4] that f is a *Morse function*, i.e., such that its critical points (i.e., the points of $\mathbb{R}^N$ where the differential *df* vanishes) are isolated. One of the most important results of Morse theory is that the topology of the hypersurfaces $f^{-1}(u)$ can change *only* by crossing a critical level $f^{-1}(u_c)$, i.e., a level set containing at least one critical point of f. This means that a generic change in the topology of the hypersurfaces can be associated with critical points of f. Now, the hypersurfaces $f^{-1}(u)$ can be given a Riemannian metric in a standard way [197], and it is possible to analyze the behavior of the curvature fluctuations in a neighborhood of a critical point. Let us assume, for the sake of simplicity,

[4] This is not a strong assumption: in fact, it can be shown that Morse functions are generic (see Appendix C).

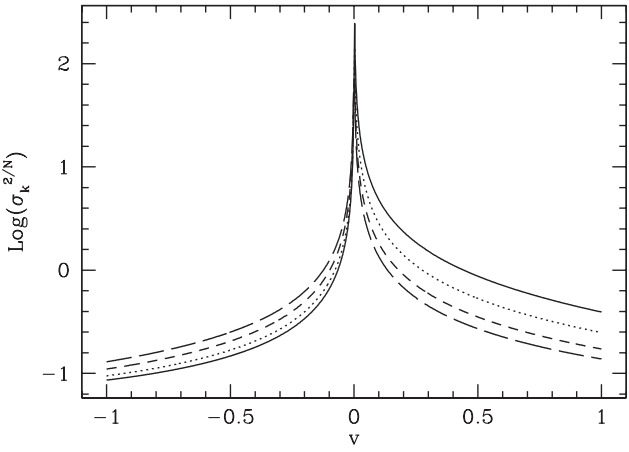

Fig. 7.3. Fluctuations of the Gauss curvature of a hypersurface $f^{-1}(u)$ of $\mathbb{R}^N$ vs. u close to a critical point. Here $\sigma_k^{2/N}$ is reported because it has the same dimensions of the scalar curvature. Also $\dim(f^{-1}(u)) = 100$, and the Morse indexes are $1, 15, 33, 48$, represented by solid, dotted, dashed, and long-dashed lines respectively. From [194].

that this critical point is located at $x_0 = 0$ and belongs to the level $u_c = 0$. Any Morse function can be parametrized, in the neighborhood of a x_0, by means of the so-called Morse chart, i.e., a system of local coordinates $\{y_i\}$ such that $f(y) = f(x_0) - \sum_{i=1}^{k} y_i^2 + \sum_{i=k+1}^{N} y_i^2$ (k is the Morse index of the critical point). Then standard formulas for the Gauss curvature K of hypersurfaces of $\mathbb{R}^N$ [197] can be used to compute explicitly the fluctuations of the curvature, σ_K, of the level set $f^{-1}(u)$. Numerical results for the curvature fluctuations are reported in Figure 7.3 and show that also at high dimension σ_K^2 develops a sharp, singular peak as the critical surface is approached (for computational details are reported in [195]).

7.2 Topology Changes in Configuration Space and Phase Transitions

As we have discussed in Chapter 6, the curvature fluctuations of the configuration space exhibit cusplike patterns in the presence of a second-order phase transition. A truly cuspy pattern, i.e., an analytic discontinuity, is mathematically proven in the case of mean-field XY model. In Section 7.1, we have shown that singular patterns in the fluctuations of the curvature of a Riemannian manifold can be seen as consequences of the presence of a topology change. Hence, we are led to the topological hypothesis (TH), i.e., to conjecture that

at least continuous, symmetry-breaking phase transitions are associated with topology changes in the configuration space of the system.[5]

However, an important question arises, in that the fluctuations of the curvature considered in Chapter 6 have been obtained as time averages, computed along the dynamical trajectories of the Hamiltonian systems under investigation (or as statistical averages computed analytically, as in the case of the mean-field XY model). Now, time averages of geometric observables are usually found to be in excellent agreement with ensemble averages [86, 89, 90, 92, 131], so that one could argue that the above-mentioned singular-like patterns of the fluctuations of geometric observables are simply the precursors of truly singular patterns due to the fact that the measures of all the statistical ensembles tend to become singular in the limit $N \to \infty$ when a phase transition is present. In other words, geometric observables, like any other "honest" observable, already at finite N would feel the eventually singular character of the statistical measures, i.e., of the probability distribution functions of the statistical-mechanical ensembles. If this were the correct explanation, we could not attribute the cusplike patterns of the curvature fluctuations to any special geometric features of configuration space, and the cusp-like patterns observed in the numerical simulations could not be considered as (indirect) confirmations of the TH.

In order to elucidate this important point, three different paths have been followed: (i) *purely geometric* information about certain submanifolds of configuration space has been worked out *independently* of the statistical measures in the case of the two-dimensional φ^4 model, and the results lend *indirect* support to the TH [194]; (ii) a *direct* numerical confirmation of the TH has been given in [198] by means of the computation of a topologic invariant, the Euler characteristic, in the case of a 2D lattice φ^4 model; (iii) a *direct* analytic confirmation of the TH has been found in the particular case of the mean-field XY model [199] and of a trigonometric model with k-body interactions. We report on items (i) and (ii) in this chapter and (iii) in Chapter 10.

7.3 Indirect Numerical Investigations of the Topology of Configuration Space

In order to separate the singular effects due to the singular character of statistical measures at a phase transition from the singular effects due to some topological transition in configuration space, the first natural step is to consider again σ_K^2 as an observable, and to integrate it on suitable submanifolds of configuration space by means of a geometric measure, i.e., by means of a measure that has nothing to do with statistical ensemble measures.

Consider as ambient space the N-dimensional configuration space M of a Hamiltonian system with N degrees of freedom, which, when $N \to \infty$,

[5] As we shall see in the following chapters, also first-order phase transitions are necessarily driven by topological changes.

undergoes a phase transition at a certain finite temperature T_c (or critical energy per degree of freedom ε_c), and let $V(\varphi)$ be its potential energy.

Then the relevant geometrical objects are the submanifolds of M defined by

$$M_u = V^{-1}(-\infty, u] = \{\varphi \in M : V(\varphi) \leq u\} \ , \tag{7.8}$$

i.e., each M_u is the set $\{\varphi_i\}_{i=1}^N$ such that the potential energy does not exceed a given value u. As u is increased from $-\infty$ to $+\infty$, this family covers successively the whole manifold M. All the submanifolds M_u can be given a Riemannian metric g whose choice is largely arbitrary. On all these manifolds (M_u, g) there is a standard invariant volume measure:

$$d\eta = \sqrt{\det(g)}\, d\varphi_1 \cdots d\varphi_N \ , \tag{7.9}$$

which has nothing to do with statistical measures. Let us finally define the hypersurfaces Σ_u as the u-level sets of V, i.e.,

$$\Sigma_u = V^{-1}(u) \ , \tag{7.10}$$

which are nothing but the boundaries of the submanifolds M_u.

According to the discussion reported in Section 7.1, an indirect way to study the presence of topology changes in the family $\{(M_u, g)\}$ is to look at the behavior of the fluctuations of the Gaussian curvature, σ_K^2, defined as

$$\sigma_K^2 = \langle K_G^2 \rangle_{\Sigma_u} - \langle K_G \rangle_{\Sigma_u}^2 \ , \tag{7.11}$$

where $\langle \cdot \rangle$ stands for integration over the surface Σ_u, as a function of u. The presence of cusplike singularities of σ_K^2 for some critical value of u, u_c, would eventually signal the presence of a topology change of the family $\{(M_u, g)\}$ at u_c [194]. Such an indirect geometric probing of the presence of critical points seems an expedient way to probe the possible topology changes of the manifolds (M_u, g). In fact, the properties of the manifolds M_u are closely related to those of the hypersurfaces $\{\Sigma_u\}_{u \leq u_c}$, as can be inferred from the equation

$$\int_{M_u} f d\eta = \int_0^u dv \int_{\Sigma_v} f|_{\Sigma_v} d\omega / \|\nabla V\| \ , \tag{7.12}$$

where $d\omega$ is the induced measure[6] on Σ_u and f a generic function [200]. From Morse theory (see Appendix C) we know that the surface Σ_{u_c} defined by $V = u_c$ is a degenerate quadric, so that in its vicinity some of the principal curvatures [197] of the surfaces $\Sigma_{u \approx u_c}$ tend to diverge.[7] Such a divergence

[6] If a surface is parametrically defined through the equations $x^i = x^i(z^1, \ldots, z^k)$, $i = 1, \ldots, N$, then the metric g_{ij} induced on the surface is given by $g_{ij}(z^1, \ldots, z^k) = \sum_{n=1}^N \frac{\partial x^n}{\partial z^i} \frac{\partial x^n}{\partial z^j}$. See Appendix B.

[7] The principal curvatures are the inverse of the curvature radii measured, at any given point of a surface, in suitable directions. At a Morse critical point some of these curvature radii vanish.

is generically detected by any function of the principal curvatures, and thus for practical computational reasons, instead of the Gauss curvature (which is the product of all the principal curvatures) we shall consider the total second variation of the *scalar* curvature $\mathcal{R}$ (i.e., the sum of all the possible products of two principal curvatures) of the manifolds (M_u, g), according to the definition

$$\sigma^2_{\mathcal{R}}(u) = [\mathrm{Vol}(M_u)]^{-1} \int_{M_u} d\eta \left[\mathcal{R} - [\mathrm{Vol}(M_u)]^{-1} \int_{M_u} d\eta\, \mathcal{R}\right]^2 \tag{7.13}$$

with $\mathcal{R} = g^{kj} R^l_{klj}$, where R^l_{kij} are the components of the Riemann curvature tensor [see Appendix B] and $\mathrm{Vol}(M_u) = \int_{M_u} d\eta$. The subsets M_u of configuration space are given the structure of Riemannian manifolds (M_u, g) by endowing all of them with the *same* metric tensor g. However, the choice of the metric g is arbitrary in view of probing possible effects of the topology on the geometry of these manifolds.

What has been hitherto discussed now requires the choice of a model to perform a numerical investigation. A good candidate is represented by the so-called φ^4 model on a d-dimensional lattice $\mathbb{Z}^d$ with $d = 1, 2$, described by the potential function

$$V = \sum_{i \in \mathbb{Z}^d} \left(-\frac{\mu^2}{2} \varphi_i^2 + \frac{\lambda}{4} \varphi_i^4 \right) + \sum_{\langle ik \rangle \in \mathbb{Z}^d} \frac{1}{2} J (\varphi_i - \varphi_k)^2 \,, \tag{7.14}$$

where $\langle ik \rangle$ stands for nearest-neighbor sites. This system has a discrete $\mathbb{Z}_2$-symmetry and short-range interactions; therefore, in $d = 1$ there is no phase transition whereas in $d = 2$ there is a symmetry-breaking transition, at a finite temperature, of the same universality class of the 2D Ising model. In [194], three different types of metrics have been considered for this model, i.e.,

(*i*) $g^{(1)}_{\mu\nu} = [A - V(\varphi)]\delta_{\mu\nu}$, i.e., a conformal deformation (Section B.3.2) of the Euclidean flat metric $\delta_{\mu\nu}$, where $A > 0$ is an arbitrary constant chosen large enough to be sure that in the relevant interval of values of u the determinant of the metric is always positive;

(*ii*) $g^{(2)}_{\mu\nu}$ and $g^{(3)}_{\mu\nu}$ are generic metrics (no longer conformal deformations of the flat metric) defined by

$$(g^{(k)}_{\mu\nu}) = \begin{pmatrix} f^{(k)} & 0 & 1 \\ 0 & \mathbb{I} & 0 \\ 1 & 0 & 1 \end{pmatrix} \quad , \qquad k = 2, 3 \,, \tag{7.15}$$

where $\mathbb{I}$ is the $(N-2)$-dimensional identity matrix, $g^{(2)}$ is obtained by setting $f^{(2)} = \frac{1}{N} \sum_{\alpha \in \mathbf{Z}^d} \varphi^4_\alpha + A$, and $g^{(3)}$ by setting $f^{(3)} = \frac{1}{N} \sum_{\alpha \in \mathbb{Z}^d} \varphi^6_\alpha + A$, with $A > 0$, and α labels the N lattice sites of a linear chain ($d = 1$) or of a square lattice ($d = 2$, $N = n \times n$).

These choices are completely arbitrary, however, and only if metrics of very simple form are chosen are both analytical and numerical computations feasible also for rather large values of N. Thus the first metric has been chosen diagonal, and the other two metrics concentrate in only one matrix element all the nontrivial geometric information. Moreover, the first metric still contains a reference to the physical potential, whereas the other two define metric structures that are completely independent of the physical potential and contain only monomials of powers sufficiently high that they do not vanish after two successive derivatives have been taken (needed to compute curvatures). The topology of the subsets of points M_u and Σ_u of $\mathbb{R}^N$ is already determined (though well concealed) by the definitions of (7.8) and (7.10); the task is to "capture" some information about their topology through a mathematical object or structure, defined on these sets of points, that is capable of mirroring the variations of topology through the u-pattern of an analytic function. This idea follows the philosophy of standard mathematical theories of differential topology. For example, within Morse theory, the information about topology is extracted through the critical points of any function—defined on a given manifold—satisfying some conditions (necessary to be a good Morse function, see Appendix C), or, within cohomology theory, topology is probed through vector spaces of differential forms (the de Rham cohomology vector spaces, see Appendix A) "attached" to a given manifold. Provided that good mathematical quantities are chosen as topology-variation detectors, arbitrary Riemannian metric structures could work as well.

For the above-defined metrics $g^{(k)}$, $k = 1, 2, 3$, simple algebra leads from the definition of the scalar curvature (see Appendix B) to the following explicit expressions:

$$\mathcal{R}^{(1)} = (N-1)\left[\frac{\triangle V}{(A-V)^2} - \frac{\|\nabla V\|^2}{(A-V)^3}\left(\frac{N}{4} - \frac{3}{2}\right)\right] , \tag{7.16}$$

$$\mathcal{R}^{(k)} = \frac{1}{(f^{(k)}-1)}\left[\frac{\|\tilde{\nabla} f^{(k)}\|^2}{2(f^{(k)}-1)} - \tilde{\triangle} f^{(k)}\right] , \quad k = 2, 3 , \tag{7.17}$$

where ∇ and $\triangle$ are the Euclidean gradient and Laplacian respectively, and $\tilde{\nabla}$ and $\tilde{\triangle}$ lack the derivative $\partial/\partial\varphi_\alpha$ with $\alpha = 1$ in the $d = 1$ case, and lack the derivative $\partial/\partial\varphi_\alpha$ with $\alpha = (1, 1)$ in the $d = 2$ case.

The numerical computation of the geometric integrals in (7.13) is worked out by means of a Monte Carlo algorithm [169, 195] to sample the geometric measure $d\eta$ by means of an "importance sampling" algorithm suitably modified (see Section 7.6.1).

In Figures 7.4 and 7.5, $\sigma^2_{\mathcal{R}}(\overline{u})$, where $\overline{u} = u/N$, are given for the one- and two-dimensional cases obtained for two different lattice sizes with $g^{(1)}$ (Figure 7.4), and at given lattice size with $g^{(2,3)}$ (Figure 7.5). Peaks of $\sigma^2_{\mathcal{R}}(\overline{u})$ appear at a certain value $\overline{u}_c = u_c/N$, of $\overline{u}$ in the two-dimensional case, whereas only smooth patterns are found in the one-dimensional case, where no phase transition is present.

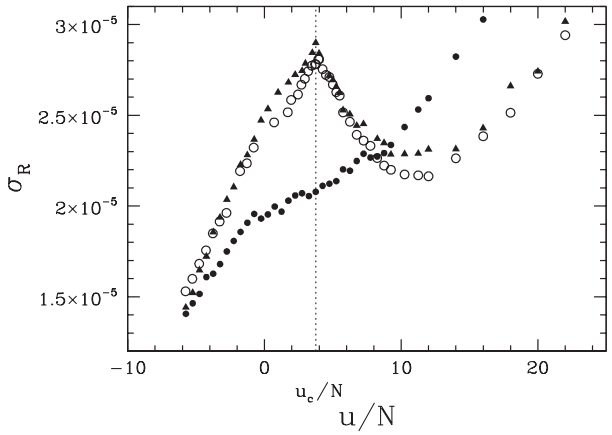

Fig. 7.4. Variance of the scalar curvature of M_u vs. u/N computed with the metric $g^{(1)}$. Full circles correspond to the 1D φ^4 model with $N = 400$. Open circles refer to the 2D φ^4 model with $N = 20 \times 20$ lattice sites, and full triangles refer to 40×40 lattice sites (whose values are rescaled for graphical reasons). From [194].

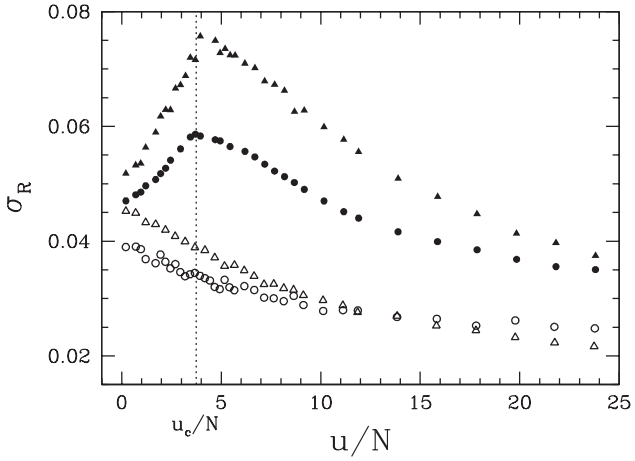

Fig. 7.5. $\sigma^2_{\mathcal{R}}(\overline{u})$ of M_u vs. u/N computed for the φ^4 model with metric $g^{(2)}$ in 1D, $N = 400$ (open triangles); metric $g^{(2)}$ in 2D, $N = 20 \times 20$ (full triangles); metric $g^{(3)}$ in 1D, $N = 400$ (open circles); metric $g^{(3)}$ in 2D, $N = 20 \times 20$ (full circles). From [194].

According to the discussion above, these peaks can be considered as indirect evidence of the presence of a topology transition in the manifolds M_u at $u = u_c$ in the case of the two-dimensional φ^4 model. It is in particular the persistence of cusplike patterns of $\sigma^2_{\mathcal{R}}(\overline{u})$ independently of the metric chosen that lends credence to the idea that this actually reflects a topological transition. Now we want to argue that the topological transition occurring at

u_c/N is related to a *thermodynamic phase transition* that occurs in the φ^4 model. In order to do that, in [194] the average potential energy per particle

$$\frac{u(T)}{N} = \frac{\langle V \rangle}{N} \tag{7.18}$$

has been numerically computed, as a function of T, by means of both Monte Carlo averaging with the canonical configurational measure and Hamiltonian dynamics. In the latter case the temperature T is given by the average kinetic energy per degree of freedom, and u is obtained as the time average. Figure 7.6 shows a perfect agreement between time and ensemble averages. The phase transition point is well visible at $\overline{u}_c = u_c/N \approx 3.75$. Looking at Figures 7.4 and 7.5, we realize that within the numerical accuracy, the critical value of the potential energy per particle u_c/N where the topological change occurs equals the statistical-mechanical average value of the potential energy at the phase transition. At this point the doubt, formulated at the beginning of this chapter, about the possible nongeometrical origin of the "singular" cusplike patterns of $\sigma^2_{\mathcal{R}}(\overline{u})$ has been dissipated. These results have been found *independently* of statistical-mechanical measures and of their singular character in the presence of a phase transition. These results are also *independent*—at least to the limited extent of the three metric tensors reported above—of the geometric structure given to the family $\{M_u\}$. Thus they seem most likely to have their origin at a deeper level than the geometric one, i.e. at the topologic level. Hence the observed phenomenology strongly hints that some *major* change in the topology of the configuration-space submanifolds $\{M_u\}$ occurs when a second-order phase transition takes place.

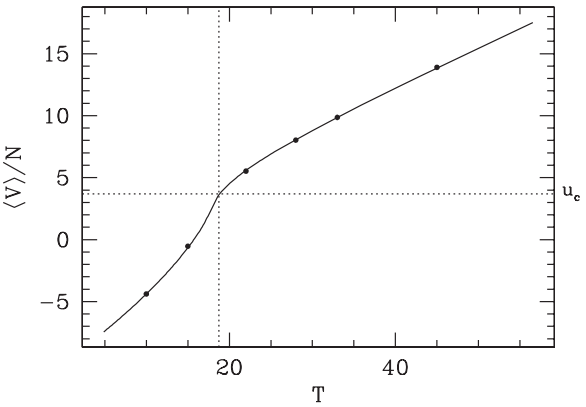

Fig. 7.6. Average potential energy vs. temperature for the 2D lattice φ^4 model with $O(1)$ symmetry. Lattice size $N = 20 \times 20$. The solid line is made out of 200 points obtained as time averages. Full circles represent Monte Carlo estimates of canonical ensemble averages. The dotted lines locate the phase transition. From [194].

7.4 Topological Origin of the Phase Transition in the Mean-Field *XY* Model

Until now we have not yet given any *direct* analytic evidence of the validity of the TH. Let us now consider again the mean-field XY model (6.13). As we shall see in detail in Chapter 10, for this model we can analytically compute both its thermodynamics and a topological invariant (the Euler–Poincaré characteristic) of the submanifolds M_v of its configuration space. Hence, it is possible to show analytically that a particular topological change in the configuration space is related to the thermodynamic phase transition. However, in this chapter we begin by discussing a first simplified approach to the model [199] giving evidence of the topological transition in a space of collective variables.

Let us consider again, as was already done in Section 7.3, the family M_v of submanifolds of the configuration space defined in (7.8); now the potential energy per degree of freedom is that of the mean-field XY model, i.e.,

$$\mathcal{V}(\varphi) = \frac{V(\varphi)}{N} = \frac{J}{2N^2} \sum_{i,j=1}^{N} [1 - \cos(\varphi_i - \varphi_j)] - \frac{h}{N} \sum_{i=1}^{N} \cos \varphi_i \ , \tag{7.19}$$

where $\varphi_i \in [0, 2\pi]$. Such a function can be considered a Morse function on M, so that, according to Morse theory (see Appendix C), all these manifolds have the same topology until a critical level $\mathcal{V}^{-1}(v_c)$ is crossed, where the topology of M_v changes.

A change in the topology of M_v can occur only when v passes through a critical value of $\mathcal{V}$. Thus in order to detect topological changes in M_v we have to find the critical values of $\mathcal{V}$, which means solving the equations

$$\frac{\partial \mathcal{V}(\varphi)}{\partial \varphi_i} = 0 \ , \qquad i = 1, \ldots, N \ . \tag{7.20}$$

For a general potential energy function $\mathcal{V}$, the solution of the (7.20) would be a formidable task [202], but in the case of the mean-field XY model, the mean-field character of the interaction greatly simplifies the analysis, allowing an analytical treatment of the (7.20); moreover, a projection of the configuration space onto a two-dimensional plane is possible.

We recall that in the limit $h \to 0$, the system has a continuous phase transition, with classical critical exponents, at $T_c = 1/2$, or $\varepsilon_c = 3/4$, where $\varepsilon = E/N$ is the energy per particle. Let us now show that this phase transition has its foundation in a basic topological change that occurs in the configuration space M of the system. To begin with, note that since $\mathcal{V}(\varphi)$ is bounded, $-h \leq \mathcal{V}(\varphi) \leq 1/2 + h^2/2$, the manifold is empty as long as $v < -h$, and when v increases beyond $1/2 + h^2/2$ no changes in its topology can occur, so that the manifold M_v remains the same for any $v > 1/2 + h^2/2$, and is then an N-torus. To detect topological changes we have to solve (7.20). To this end

it is useful to define the magnetization vector, i.e., the collective spin vector $\mathbf{m} = \frac{1}{N}\sum_{i=1}^{N} \mathbf{s}_i$, which as a function of the angles is given by

$$\mathbf{m} = (m_x, m_y) = \left(\frac{1}{N}\sum_{i=1}^{N} \cos\varphi_i, \frac{1}{N}\sum_{i=1}^{N} \sin\varphi_i \right) . \tag{7.21}$$

Due to the mean-field character of the model, the potential energy (6.13) can be expressed as a function of $\mathbf{m}$ alone (remember that $J = 1$), so that the potential energy per particle reads

$$\mathcal{V}(\varphi) = \mathcal{V}(m_x, m_y) = \frac{1}{2}(1 - m_x^2 - m_y^2) - h\, m_x . \tag{7.22}$$

This allows us to write (7.20) in the form ($i = 1, \ldots, N$)

$$(m_x + h)\sin\varphi_i - m_y \cos\varphi_i = 0 . \tag{7.23}$$

Now we can solve these equations and find all the critical values of $\mathcal{V}$. The solutions of (7.23) can be grouped into three classes:

(i) The minimal energy configuration $\varphi_i = 0\ \forall i$, with a critical value $v = v_0 = -h$, which tends to 0 as $h \to 0$. In this case, $m_x^2 + m_y^2 = 1$.

(ii) Configurations such that $m_y = 0, \sin\varphi_i = 0\ \forall i$. These are the configurations in which φ_i equals either 0 or π; i.e., we have again $\varphi_i = 0\ \forall i$, but also the N configurations with $\varphi_k = \pi$ and $\varphi_i = 0\ \forall i \neq k$, as well as the $N(N-1)$ configurations with 2 angles equal to π and all the others equal to 0, and so on, up to the configuration with $\varphi_i = \pi\ \forall i$. The critical values corresponding to these critical points depend only on the number of π's, n_π, so that $v(n_\pi) = \frac{1}{2}[1 - \frac{1}{N^2}(N - 2n_\pi)^2] - \frac{h}{N}(N - 2n_\pi)$. We see that the largest critical value is, for N even, $v(n_\pi = N/2) = 1/2$ and that the number of critical points corresponding to it is $\mathcal{O}(2^N)$.

(iii) Configurations such that $m_x = -h$ and $m_y = 0$, which correspond to the critical value $v_c = 1/2 + h^2/2$, which tends to $1/2$ as $h \to 0$. The number of these configurations grows with N not slower than $N!$ [199].

Configurations (i) are the absolute minima of $\mathcal{V}$, (iii) are the absolute maxima, and (ii) are all the other stationary configurations of $\mathcal{V}$.

Since for $v < v_0$ the manifold is empty, the topological change that occurs at v_0 is the one corresponding to the "birth" of the manifold from the empty set; subsequently there are many topological changes at values $v(n_\pi) \in (v_0, 1/2]$ till at v_c there is a final topological change that corresponds to the "completion" of the manifold. We remark that the number of critical values in the interval $[v_0, 1/2]$ grows with N and that eventually the set of these critical values becomes dense in the limit $N \to \infty$. However, the critical value v_c remains isolated from other critical values also in that limit. We observe that it is necessary to consider a nonzero external field h in order that $\mathcal{V}$ be a Morse function, because if $h = 0$ all the critical points of classes (i) and (ii)

are degenerate, in which case topological changes do not necessarily occur.[8] This degeneracy is due to the $O(2)$-invariance of the potential energy in the absence of an external field. To be sure, for $h \neq 0$, $\mathcal{V}$ may not be a Morse function on the whole of M either, but only on M_v with $v < v_c$, because the critical points of class (iii) may also be degenerate, so that v_c does not necessarily correspond to a topological change. However, this difficulty could be dealt with by using that the potential energy can be written in terms of the collective variables m_x and m_y, as in (7.22). This implies that we consider the system of N spins projected onto the two-dimensional configuration space of the collective spin variables. According to the definition (7.21) of $\mathbf{m}$, the accessible configuration space is now not the whole plane, but only the disk

$$D = \{(m_x, m_y) : m_x^2 + m_y^2 \leq 1\} \ . \tag{7.24}$$

Thus we want to study the topology of the submanifolds

$$D_v = \{(m_x, m_y) \in D : \mathcal{V}(m_x, m_y) \leq v\} \ . \tag{7.25}$$

The sequence of topological transformations undergone by D_v can now be very simply determined in the limit $h \to 0$ (see Figure 7.7), as follows. As long as $v < 0$, D_v is the empty set. The first topological change occurs at $v = v_0 = 0$, where the manifold appears as the circle $m_x^2 + m_y^2 = 1$, i.e., the boundary ∂D of D. Then as v grows D_v is given by the conditions

$$1 - 2v \leq m_x^2 + m_y^2 \leq 1 \ , \tag{7.26}$$

i.e., it is the ring with a hole centered at $(0, 0)$ (punctured disk) contained between two circles of radii 1 and $\sqrt{2v}$. As v continues to grow, the hole shrinks and is eventually completely filled when $v = v_c = 1/2$, where the second topological change occurs (see Section A.5 on the fundamental group). In this coarse-grained two-dimensional description in D, all the topological

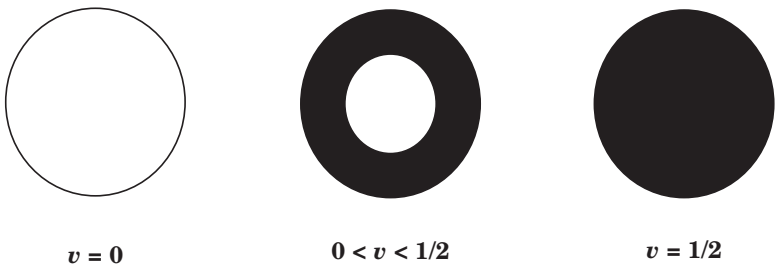

Fig. 7.7. The sequence of topological changes undergone by the manifolds D_v with increasing v in the limit $h \to 0$.

[8] It would also be possible to avoid this problem by considering an improved version of Morse theory, referred to as *equivariant Morse theory* [203].

changes that occur in M between $v = 0$ and $v = 1/2$ disappear, and only the two topological changes corresponding to the extrema of $\mathcal{V}$, occurring at $v = v_0$ and $v = v_c$, survive. This means that the topological change at v_c should be present also in the full N-dimensional configuration space, so that the degeneracies mentioned above for the critical points of class (iii) should not prevent a topological change.

Now we want to argue that the topological change occurring at v_c is related to the thermodynamic phase transition of the mean-field XY model. Since the Hamiltonian is of the standard form (1.1), the temperature T, the energy per particle ε, and the average potential energy per particle $\overline{u} = \langle \mathcal{V} \rangle$ obey, in the thermodynamic limit, the following equation:

$$\varepsilon = \frac{T}{2} + \overline{u}(T) \ , \tag{7.27}$$

where we have set Boltzmann's constant equal to 1. Substituting the values of the critical energy per particle $\varepsilon_c = 3/4$ and of the critical temperature $T_c = 1/2$ we get $\overline{u}_c = \overline{u}(T_c) = 1/2$, so that the critical value of the potential energy per particle v_c where the last topological change occurs equals the statistical-mechanical average value of the potential energy at the phase transition,

$$v_c = \overline{u}_c \ . \tag{7.28}$$

Thus although a topological change in M occurs at any N, and v_c is *independent* of N, there is a connection of such a topological change and a thermodynamic phase transition *only* in the limit $N \to \infty$, $h \to 0^+$, when indeed a thermodynamic phase transition can be defined.

Since *not all* topological changes correspond to phase transitions, those that do correspond remain to be determined to make the conjecture of [92] more precise. In this context, we consider one example where there are topological changes very similar to the ones of our model but no phase transitions, i.e., the one-dimensional XY model with nearest-neighbor interactions, whose Hamiltonian is of the class (1.1) with interaction potential

$$V(\varphi) = \frac{1}{4} \sum_{i=1}^{N} [1 - \cos(\varphi_{i+1} - \varphi_i)] - h \sum_{i=1}^{N} \cos \varphi_i \ . \tag{7.29}$$

In this case the configuration space M is still an N-torus, and using again the potential energy per degree of freedom $\mathcal{V} = V/N$ as a Morse function, we can see that also here there are many topological changes in the submanifolds M_v as v is varied in the interval $[0, 1/2]$ (after taking $h \to 0^+$). However there are critical points of the type $\varphi_j = \varphi_k = \varphi_l = \cdots = \pi$, $\varphi_i = 0 \ \forall i \neq j, k, l, \ldots$; in contrast to the mean-field XY model, it is now no longer the number of π's that determines the value of $\mathcal{V}$ at the critical point, but rather the number of domain walls, n_d, i.e., the number of boundaries between "islands" of π's and "islands" of 0's: $v(n_d) = n_d/2N$. Since $n_d \in [0, N]$, the critical values lie in the

same interval as in the case of the mean-field XY model; but now the maximum critical value $v = 1/2$, instead of corresponding to a huge number of critical points, which rapidly grows with N, corresponds to *only two* configurations with N domain walls, which are $\varphi_{2k} = 0$, $\varphi_{2k+1} = \pi$, with $k = 1, \ldots, N/2$, and the reversed one. There are also "spin-wave-like" critical points, i.e., such that $e^{i\theta_k} = \text{const}\ e^{2\pi i k n/N}$ with $n = 1, \ldots, N$ [204]; their critical energies are contained in the interval above but again there is not a critical value associated with a huge number of critical points.

Thus this example suggests the conjecture that a topological change in the configuration-space submanifolds M_v occurring at a critical value v_c is associated with a phase transition in the thermodynamic limit only if the number of critical points corresponding to the critical value v_c is sufficiently rapidly growing with N and makes a big jump at v_c. On the basis of the behavior of the mean-field XY model we expect then that such a growth should be at least exponential. Furthermore, a relevant feature appears to be that v_c remains an isolated critical value also in the limit $N \to \infty$: in the mean-field XY model this holds only if the thermodynamic limit is taken *before* the $h \to 0^+$ limit: this appears as a topological counterpart of the noncommutativity of the limits $h \to 0^+$ and $N \to \infty$ in order to get a phase transition in statistical mechanics.

The sequence of topological changes occurring with growing $\mathcal{V}$ makes the configuration space larger and larger, till at v_c the whole configuration space becomes fully accessible to the system through the last topological change. From a physical point of view, this corresponds to the appearance of more and more disordered configurations as T grows, which ultimately lead to the phase transition at T_c.

7.5 The Topological Hypothesis

Let us consider the canonical partition function Z_N for an N-degrees-of-freedom system described by a standard Hamiltonian $H(p, q) = \sum p^2/2 + V(q)$, where p and q are vectors. For these systems, after a trivial integration of the kinetic energy term, it reads

$$Z(\beta, N) = \int d^N p\ d^N q\ e^{-\beta H(p,q)} = \left(\frac{\pi}{\beta}\right)^{\frac{N}{2}} \int d^N q\ e^{-\beta V(q)}\,, \qquad (7.30)$$

showing that its nontrivial part is the configurational partition function

$$Z_c(\beta, N) = \int_{\mathbb{R}^N} d^N q\ e^{-\beta V(q)} = \int_0^{+\infty} dv\ e^{-\beta v} \int_{\Sigma_v} \frac{d\sigma}{\|\nabla V\|}\,, \qquad (7.31)$$

where a coarea formula [200] has been used to unfold the *structure integrals*

$$\Omega_N(v) \equiv \int_{\Sigma_v} \frac{d\sigma}{\|\nabla V\|} \quad , \tag{7.32}$$

an infinite collection of integrals on the *equipotential hypersurfaces* Σ_v of the configuration space defined by $\Sigma_v \equiv \{q \in \mathbb{R}^N | V(q) = v\} \subset \mathbb{R}^N$, and $d\sigma$ is the volume form induced by the immersion of Σ_v in $\mathbb{R}^N$.

Equation (7.31) shows that, formally, Z_c is the Laplace transform of the structure integral.

Then, if we consider the *microcanonical* ensemble, the basic mathematical object is the phase space volume

$$\Omega(E) = \int_0^E d\eta \; \Omega^{(-)}(E-\eta) \; \int d^N p \; \delta\left(\sum_i \frac{1}{2} p_i^2 - \eta\right)$$

where

$$\Omega^{(-)}(E-\eta) = \int d^N q \; \Theta[V(q) - (E-\eta)] = \int_0^{E-\eta} dv \; \int_{\Sigma_v} \frac{d\sigma}{\|\nabla V\|} \; , \tag{7.33}$$

whence

$$\Omega(E) = \int_0^E d\eta \; \frac{(2\pi\eta)^{N/2}}{\eta \Gamma(\frac{N}{2})} \int_0^{E-\eta} dv \; \int_{\Sigma_v} \frac{d\sigma}{\|\nabla V\|} \; . \tag{7.34}$$

Here too, as in the above decomposition of $Z_c(\beta, N)$, the only nontrivial objects are the structure integrals (7.32).

Once the microscopic interaction potential $V(q)$ is given, the configuration space of the system is *automatically* foliated into the family $\{\Sigma_v\}_{v \in \mathcal{R}}$ of equipotential hypersurfaces *independently* of any statistical measure we may wish to use. Now, from standard statistical-mechanical arguments we know that the larger the number N of particles, the closer to some Σ_v are the microstates that significantly contribute to the statistical averages of thermodynamic observables. At large N, and at any given value of the inverse temperature β, the effective support of the canonical measure is narrowed very close to a single $\Sigma_v = \Sigma_{v(\beta_c)}$; similarly, in the microcanonical ensemble, the fluctuations of potential and kinetic energies tend to vanish at increasing N so that the effective contributions to $\Omega(E)$ come from a close neighborhood of a $\Sigma_v = \Sigma_{v(E_c)}$.

Now, the *topological hypothesis* consists in assuming that some suitable change of the topology of the $\{\Sigma_v\}$, occurring at some $v_c = v_c(\beta_c)$ (or $v_c = v_c(E_c)$), is the deep origin of the singular behavior of thermodynamic observables at a phase transition (by change of topology we mean that $\{\Sigma_v\}_{v<v_c}$ are *not diffeomorphic* to the $\{\Sigma_v\}_{v>v_c}$). In other words, the claim is that the canonical and microcanonical measures must "feel" a big and sudden change, if any, of the topology of the equipotential hypersurfaces of

their underlying supports, the consequence being the appearance of the typical signals of a phase transition, i.e., almost singular energy or temperature dependencies of the averages of appropriate observables. The larger N the narrower is the effective support of the measure and hence the sharper can be the mentioned signals. Eventually, in the $N \to \infty$ limit this sharpening will lead to nonanalyticity.

On the basis of this and what was found in [92,194,199], we formulate the TH as follows:

Topological Hypothesis*: The basic origin of a phase transition lies in a topological change of the support of the measure describing a system. This change of topology induces a change of the measure itself at the transition point.*

In other words, this hypothesis stipulates that some change of the topology of the $\{\Sigma_v\}$, occurring at some $v_c = v_c(\beta_c)$, could be the origin of the singular behavior of thermodynamic observables at a phase transition rather than measure singularities, which in this view are induced from a deeper level where the topological changes take place.

Remark 7.1. As we shall see in the following chapters, topological changes of the manifolds Σ_v and M_v are associated to the existence of critical points of the potential function, i.e., points where $\nabla V = 0$. By looking at the definition of the structure integral (7.32), one could naively infer that since the denominator $\|\nabla V\|$ vanishes at the critical points, entailing a divergence of the structure integral, the critical points, and thus topology, must be relevant to the divergence of thermodynamic observables. However, such a kind of reasoning would be completely wrong and misleading. On large–N hypersurfaces the integration measure regularizes the structure integral also at the critical points so that the vanishing of the denominator does not entail any divergence of the structure integral (Consider, for example, that Σ_v is a large–N hypersphere, and write ∇V near a critical point as a quadratic form using the Morse chart). The way topology induces the appearance of thermodynamic singularities is by far more subtle, as will be clarified in the next chapters.

7.6 Direct Numerical Investigations of the Topology of Configuration Space

The first successful attempt at obtaining a direct evidence that topological changes are associated with phase transitions, and thus the first direct evidence supporting the topological hypothesis, is numerical.

Since the counterpart of a phase transition is expected to be a suitable breaking of diffeomorphicity among the surfaces Σ_v, it is appropriate to choose a *diffeomorphism invariant* to probe whether and how the topology of the Σ_v changes as a function of v. This is a very challenging task because one has to deal with high-dimensional manifolds. Fortunately, a topological invariant

exists whose computation is feasible, yet demands a big effort. This is the *Euler characteristic*, a diffeomorphism invariant, expressing fundamental topological information (see Appendix A).

Let us recall how it is defined. First, let us consider that a basic way to analyze a geometrical object is to fragment it into other more familiar objects and then to examine how these pieces fit together. Take, for example, a surface Σ in Euclidean three-dimensional space. Slice Σ into pieces that are curved triangles (this is called a triangulation of the surface). Then count the number F of faces of the triangles, the number E of edges, and the number V of vertices on the tesselated surface. Now, no matter how we triangulate a compact surface Σ, $\chi(\Sigma) = F - E + V$ will always equal a constant that is characteristic of the surface and that is invariant under diffeomorphisms $\phi : \Sigma \to \Sigma'$. This is the Euler characteristic of Σ. At higher dimensions this can be again defined by using higher-dimensional generalizations of triangles (simplices) and by defining the Euler characteristic of the n-dimensional manifold Σ to be

$$\chi(\Sigma) = \sum_{k=0}^{n} (-1)^k (\#\text{ of "faces of dimension k"}). \tag{7.35}$$

In differential topology an equivalent definition of $\chi(\Sigma)$ is

$$\chi(\Sigma) = \sum_{k=0}^{n} (-1)^k b_k(\Sigma) \ , \tag{7.36}$$

where the numbers b_k, the Betti numbers of Σ, are diffeomorphism invariants (see Appendix A). While it would be hopeless to try to compute $\chi(\Sigma)$ from (7.36) in the case of nontrivial physical models at large dimension, there is a possibility given by a powerful theorem, the Gauss–Bonnet–Hopf theorem, that relates $\chi(\Sigma)$ to the total Gauss–Kronecker curvature of the manifold, that is,

$$\chi(\Sigma) = \gamma \int_{\Sigma} K_G \, d\sigma \ , \tag{7.37}$$

which is valid for even dimensional hypersurfaces of Euclidean spaces $\mathbb{R}^N$ [here $\dim(\Sigma) = n \equiv N - 1$], and where: $\gamma = 2/\mathrm{Vol}(\mathbb{S}^n_1)$ is twice the inverse of the volume of an n-dimensional sphere of unit radius; K_G is the Gauss–Kronecker curvature of the manifold; $d\sigma = \sqrt{\det(g)} dx^1 dx^2 \cdots dx^n$ is the invariant volume measure of Σ, and g is the Riemannian metric induced from $\mathbb{R}^N$. The definition and significance of the Gauss–Kronecker curvature are given in Chapter 8. The practical computation of K_G at any point $x \in \Sigma_v$ proceeds from the knowledge of a basis $\{\mathbf{v}_1, \ldots, \mathbf{v}_n\}$ for the tangent space of Σ_v at x, so that, using the directional derivatives $\nabla_{\mathbf{v_i}} V$, it is

$$K_G(x) = \frac{(-1)^n}{\|\nabla V\|^n} \left| \begin{pmatrix} \nabla_{\mathbf{v}_1} \nabla V \\ \vdots \\ \nabla_{\mathbf{v}_n} \nabla V \\ \nabla V \end{pmatrix} \right| \left| \begin{pmatrix} \mathbf{v}_1 \\ \vdots \\ \mathbf{v}_n \\ \nabla V \end{pmatrix} \right|^{-1} \ . \tag{7.38}$$

7.6.1 Monte Carlo Estimates of Geometric Integrals

In order to perform a numerical computation of the topological invariant given by the Gauss–Bonnet–Hopf formula (7.37), the numerical evaluation of multiple integrals in high-dimensional spaces is needed. To this end, the Monte Carlo–Metropolis method was devised a long time ago and apart from a large number of improvements and modifications of the basic scheme to fit it to different kinds of problems, the main feature remains unaltered: we can compute only densities and not the actual numerical value of the multiple integral under examination. The basic scheme consists in any algorithm capable of generating a Markov chain, in the high-dimensional space of interest, whose asymptotic probability density coincides with the measure of the integral to compute.

In particular, since we have to compute surface integrals $\int_{\Sigma_v} g \; d\sigma$, it is necessary to devise an efficient algorithm to generate a Markov chain on a hypersurface. In order to constrain a Markov chain generated with the standard "importance sampling" [205] on a given Σ_v, one has to adopt a projection algorithm.

Suppose that $x_k \in \Sigma_v$ is the point generated at the kth step of the Monte Carlo Markov chain, and that the updated point at the following step $\tilde{x}_{k+1} = x_k + \Delta x_k$ is not too far from the preceding one ($\|\Delta x_k\| \ll 1$ in convenient units). In general, it is $\tilde{x}_{k+1} \in \Sigma_{v+\Delta v}$; thus $\tilde{x}_{k+1}$ is projected on the tangent plane at x_k to Σ_v. The coordinates of the updated and projected configuration are thus the following:

$$x_{k+1} = x_k - \frac{\Delta v}{\|\nabla V\|^2} \cdot \nabla V \ , \tag{7.39}$$

where $\Delta v = (\tilde{x}_{k+1} - x_k) \cdot \nabla V$ is the difference in potential energy between the two configurations. The projection algorithm allows one to efficiently perform a random walk on a hypersurface Σ_v, provided that the new configurations proposed at each step are generated and/or preselected so as not to be too far from Σ_v.

Another important point concerns the measure $d\sigma$ entering the integral 7.37. This is the canonical volume form associated with the metric tensor $g_{\alpha\gamma}(v)$ of the hypersurface that is obtained by restricting the Euclidean metric of $\mathbb{R}^N$ to Σ_v. Thus we have

$$g_{\alpha\gamma}(v) = \delta_{\alpha\gamma} + \frac{\partial_\alpha V \partial_\gamma V}{\partial_N V \partial_N V} \ ,$$

where it is understood that $g_{\alpha\gamma}(v)$is a function of the point where it is computed. The volume form is

$$d\sigma = \prod_{i=1}^{N-1} dx_i \sqrt{|g(v)|} = \prod_{i=1}^{N-1} dx_i \frac{\|\nabla V\|}{|\partial_N V|} \quad . \tag{7.40}$$

The Monte Carlo algorithm has to be defined to sample the geometric measure (7.40) through the standard "importance sampling" method. Let $\mathcal{O}(x)$ be the observable that we want to average with the measure $\sqrt{|g(v)|}$, and let $x \in \Sigma_v$ be an arbitrary initial condition. Then one proceeds with a random update of the coordinates of x so as to obtain a new configuration $\tilde{x} = (x + \Delta x) \in \Sigma_{\tilde{v}}$ not too far from x; then the coordinates of $\tilde{x}$ are modified by projecting them according to (7.39) on Σ_v. Then the following ratio of weights is computed:

$$\zeta = \frac{\sqrt{|g(v')|}}{\sqrt{|g(v)|}} \quad . \tag{7.41}$$

If $\zeta > 1$, then the new proposed configuration is accepted; if $\zeta < 1$, then a random number $w \in [0, 1]$ is generated; and if $w < \zeta$, again the new configuration is accepted. Otherwise, it is rejected and the old configuration is counted once again. The observable $\mathcal{O}(x)$ is averaged on the set of all the accepted configurations

By means of a Monte Carlo algorithm one can estimate only *averages* of observables, that is,

$$\langle \mathcal{O} \rangle_{\mathrm{MC}}(v) = \frac{\int_{\Sigma_v} d\sigma \mathcal{O}(x)}{\int_{\Sigma_v} d\sigma} \ , \tag{7.42}$$

while we are interested in evaluating the actual values of the integral (7.37). In order to do this, we should be able to estimate the volume that appears in the denominator of (7.42). Denote by

$$\omega(v) = \int_{\Sigma_v} d\sigma \tag{7.43}$$

the volume of interest, and notice that the following identity holds:

$$\frac{d}{dv} \log \omega(v) = \frac{\omega'(v)}{\omega(v)} \ , \tag{7.44}$$

where $\omega'(v)$ stands for the first derivative of the volume (7.43) with respect to v. In the absence of critical points, Federer's derivation formula (see Chapter 8) gives

$$\omega'(v) = \int_{\Sigma_v} \frac{d\sigma}{\|\nabla V\|} \nabla \left(\frac{\nabla V}{\|\nabla V\|} \right) \ . \tag{7.45}$$

However, since we tackle potentials that are good Morse functions, the number of critical values of these potentials is finite in any finite interval of potential energy values, so that, even in the presence of critical values, (7.45) can be safely used in Monte Carlo computations. In fact, the probability of numerically falling exactly on a critical level set is zero. Moreover, the volume $\omega(v)$ and its first derivative are regular (see Theorem 9.14 of the Chapter 9). By combining (7.44) and (7.45) we get

$$\frac{d}{dv}\log\omega(v) = \frac{\displaystyle\int_{\Sigma_v}\frac{d\sigma}{\|\nabla V\|}\nabla\left(\frac{\nabla V}{\|\nabla V\|}\right)}{\displaystyle\int_{\Sigma_v} d\sigma}\ , \tag{7.46}$$

which is still in suitable form to be numerically computed through a Monte Carlo algorithm.

Let us introduce the quantity[9]

$$M_1 = \nabla\left(\frac{\nabla V}{\|\nabla V\|}\right)\ , \tag{7.47}$$

which is proportional to the *mean curvature*, and integrate (7.46) to obtain

$$\omega(v) = \omega(v_0)\exp\left\{\int_{v_0}^{v} dw\left\langle\frac{M_1}{\|\nabla V\|}\right\rangle_{\mathrm{MC}}\right\}\ , \tag{7.48}$$

so that the potential energy dependence of the volume, $\omega(v)$, is determined apart from a constant $\omega(v_0)$, which, however, is the same for any value v. This last equation makes it possible to numerically estimate, by means of a Monte Carlo algorithm, the integral (7.37), with the only indeterminacy due to the unknown multiplicative constant $\omega(v_0)$.

7.6.2 Euler Characteristic for the Lattice ϕ^4 Model

Let us now consider the family of $\{\Sigma_v\}_{v\in\mathbb{R}}$ associated again with the lattice φ^4 model, described by the potential function (7.14) and show how things work in practice.

By computing $\chi(\Sigma_v)$ vs. v according to (7.37), one can probe whether and how the topology of the hypersurfaces Σ_v varies with v. A variation of the Euler characteristic signals a change of topology. However, the converse can be false. For example, odd-dimensional manifolds have vanishing Euler characteristic no matter what their topology is. But the Euler characteristic, as far as a numerical investigation of topology is concerned, seems to be "the only game in town." So, in order to make possible the numerical estimate of the variations of the Euler characteristic, we resort to the Monte Carlo algorithm described above. By means of a Monte Carlo scheme we can estimate only $\int_{\Sigma_v} K_G\, d\sigma / \int_{\Sigma_v} d\sigma$ rather than the total value (7.37) of K_G on Σ_v, hence the need for an estimate of $\omega(v) = \int_{\Sigma_v} d\sigma$ as a function of v. This is achieved by means of formula (7.48), which requires us to compute also the Monte Carlo average $\langle M_1/\|\nabla V\|\rangle_{\mathrm{MC}}^{\Sigma_v}$. Thus the final outcome of these computations is the *relative* variation of the Euler characteristic as a function of v.

The computation of K_G at any point $x \in \Sigma_v$ proceeds by working out an orthogonal basis for the tangent space at x, orthogonal to $\boldsymbol{\xi} = \nabla V/\|\nabla V\|$,

[9] In mathematical textbooks, mean curvature is defined as $-\frac{1}{N}\nabla\left(\frac{\nabla V}{\|\nabla V\|}\right)$.

by means of a Gram–Schmidt orthogonalization procedure. Equation (7.38) is used to compute K_G at x.

In [198], K_G was computed at a number of points on each Σ_v varying between $1 \cdot 10^6$ and $3.5 \cdot 10^6$. The computations were performed for $\dim(\Sigma_v) = 48$ and $= 80$ (i.e., $N = 7 \times 7$, and 9×9) and with the choice $\lambda = 0.6$, $\mu^2 = 2$, $J = 1$ for the parameters of the potential.

In order to test the reliability of the numerical procedure to compute $\chi(\Sigma_v)$, the method is checked against a simplified form of the potential V in (7.14), i.e., with $\lambda = J = 0$, $\mu^2 = -1$. In this case the Σ_v are hyperspheres and therefore $\chi(\mathbb{S}_v^n) = 2$ for any even n. The integral $\int_{\Sigma_v} d\sigma$ is analytically known as a function of the radius $\sqrt{v}$. Therefore, the starting value $\omega(v_0) = \int_{\Sigma_{v_0}} d\sigma$ is known, and in this case we can compute the actual values of $\chi(\Sigma_v)$ instead of their relative variations only. In Figure 7.8 we report $\chi(\Sigma_v = \mathbb{S}_v^n)$ vs. v/N for $N = 5 \times 5$; the results are in agreement with the theoretical value within an error of few percent, a very good precision in view of the large variations of $\chi(\Sigma_v)$ that are found with the full expression (7.14) of V.

In Figure 7.9 we report the results for the 1D lattice, which is known not to undergo any phase transition. Apart from some numerical noise—here enhanced by the more complicated topology of the Σ_v when $\lambda, J \neq 0$—a monotonical (on average) decreasing pattern of $\chi(v/N)$ is found. Since the variation of $\chi(v/N)$ signals a topology change of the $\{\Sigma_v\}$, Figure 7.9 tells that a "smoothly" varying topology is not *sufficient* for the appearance of a phase transition. In fact, when the 2D lattice is considered, the pattern of $\chi(v/N)$ is very different: it displays a rather abrupt *change of the topology variation rate with* v/N at some v_c/N. This result is reported in Fig. 7.10 for a lattice of $N = 7 \times 7$ sites. The question is now whether the value v_c/N, at which $\chi(v/N)$ displays a cusp, has anything to do with the thermodynamic phase transition, i.e., we wonder whether the effective support of the canonical measure shrinks close to $\Sigma_{v \equiv v_c}$ just at $\beta \equiv 1/T_c$, the (inverse) critical temperature of the phase transition. The answer is in the affirmative. In fact, the numerical analysis, already discussed in this chapter, shows that

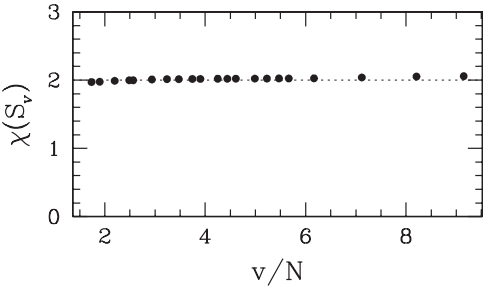

Fig. 7.8. Numerical computation of the Euler characteristic for 24-dimensional spheres. Here v is the squared radius. From [198].

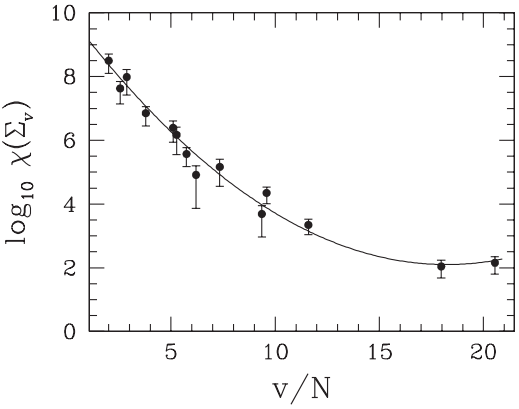

Fig. 7.9. 1D φ^4 model. Relative variations of the Euler characteristic of Σ_v vs. v/N (potential energy density). Lattice of $N = 1 \times 49$ sites. Full line is a guide to the eye. From [198].

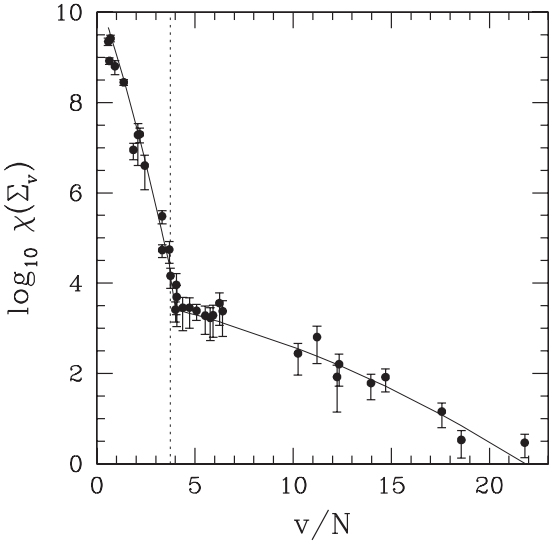

Fig. 7.10. 2D φ^4 model. Relative variations of the Euler characteristic of Σ_v vs. v/N (potential energy density). Lattice of $N = 7 \times 7$ sites. The vertical dotted line corresponds to the phase transition point. Full line is a guide to the eye. From [198].

with $\lambda = 0.6$, $\mu^2 = 2$, $J = 1$, the function $\frac{1}{N}\langle V\rangle(T)$ and its derivative signal the phase transition at $\frac{1}{N}\langle V\rangle \approx 3.75$, a value in very good agreement, within the numerical precision, with v_c/N, where the cusp of $\chi(v/N)$ shows up. We see that a sudden "*second-order variation*" of the topology of these hypersurfaces is the "suitable" topology change—mentioned at the beginning of the

present section—that underlies the phase transition of the second kind in the lattice φ^4 model.

In conclusion, through the computation of the v-dependence of a topological invariant, the hypothesis of a deep connection between topological changes of the $\{\Sigma_v\}$ and phase transitions is given *direct* confirmation.

We emphasize, and clarify in the following chapters, that not all topological transitions lead to physical phase transitions, as is clearly shown by the results given above for the 1D version of the φ^4 model. Being certain that not every topological transition corresponds to a phase transition, it seems that on the basis of the above given results, a phase transition corresponds to a supercombination of many simultaneous elementary topological transitions taking place,[10] where many might mean at least exponentially growing with the number of degrees of freedom. It seems therefore more like a supertopologically constructed transition, as will be discussed in Chapter 10.

[10] With elementary topological transition we mean any change of topology associated with a single critical point, and thus with the attachment of the corresponding handle. See Appendix C.